

EXPERIMENTAL STUDY OF THE EFFECT OF CATALYST PROPERTIES ON HYDRODYNAMICS AND MASS TRANSFER IN A SLURRY REACTOR

Mohammad Fadhil Abid,

Chemical Engineering Department
University of Technology- Iraq.
dr_mfa@uotechnology.edu.iq

Hiba Mahmood Abdullah

Chemical Engineering Department
University of Technology- Iraq.
hiba_eng26@yahoo.com

Arooba Nafa Abdullah

Chemical Engineering Department
University of Technology- Iraq.
orooba_na@yahoo.com

Abstract

This study was devoted to investigate the effect of two commonly used catalyst supports in heterogeneous catalyzed chemical reactions-e.g., silica and carbon particles- on the hydrodynamic parameters and mass transfer rate in a slurry reactor. The influence of silica and activated carbon particles concentration up to 20% v/v on regime transition, average gas holdup, mass transfer coefficient, and CO₂ removal was studied in a semi-batch slurry bubble column reactor (SBC) with a porous gas sparger. The influence of particle hydrophobicity, the influence of inorganic electrolyte (NaCl) and the combination of particle and electrolyte were also studied. It was found that hydrophobic and hydrophilic particles at concentration larger than 3 %v/v decrease the gas holdup and shift regime transition point to less gas velocity. The gas holdup increases with gas velocity, increases with electrolyte concentration, decreases with slurry concentration, and is higher for hydrophobic particles (i.e., AC particles). Experimental results show that the optical fiber probe is valid to use in a slurry bubble column and can also generate useful data such as bubble rise velocity and bubble distribution. Volumetric liquid-side mass transfer coefficient can be predicted satisfactorily by means of optical fiber probes technique within ($\pm 18\%$). Mass transfer experiments with gaseous CO₂ showed a behavior of removal in the same trend of increasing gas holdup with gas velocity. A noticeable removal of gaseous pollutants was observed for non-wettable particles at solid loading of 3%v/v. Mathematical correlations were formulated for CO₂ removal as function of studied operating variables with correlation factors of 0.95-0.98. The present study depicts the effect of catalyst carrier on the hydrodynamics and mass transfer in a slurry reactor.

Keywords: Slurry reactor, catalyst support, Hydrodynamics, particle hydrophobicity, Optical fibers, mass transfer coefficient, CO₂ removal

Introduction

One of the most alarms in global environmental problems of today is the increase in the global temperature. This problem caused by the increasing of some gases pollutants (e.g., CO₂ and CH₄) concentration from many industrial plants. To

minimize and control this effect an efficient improvement must be carried out to the absorption and reaction systems (Babadi, 2005). The slurry bubble column is used in the chemical process industries as absorbers or reactors. They are typically applied to hydrogenation, chlorination, sulfonation-reaction, Fisher-Tropsch synthesis or utilized as absorbers of environmental gaseous pollutants. Slurry bubble column reactors operate by suspending catalytic particles in a liquid and feeding gas phase reactants into the bottom of the reactor through a gas distributor which produce small bubbles. As the gas bubbles rise through the reactor, the reactants are absorbed into the liquid and diffuse to the catalyst where, depending on the catalyst system, they can be both liquid and gaseous products. If gaseous products are formed, they enter the gas bubbles and collected at the top of the reactor. A principle advantage of slurry reactors over fixed bed reactors is that the presence of a circulating / agitated slurry phase greatly increases the transfer rate of heat to cooling surfaces built into the reactor. Because reactions of interest are often highly exothermic, this results in reduced reactor cost (less heat transfer equipment is needed) and improved stability during reactor operation. A distinct advantage of bubble columns over mechanically stirred reactors is that the required mixing is effected by the action of rising bubbles, a process significantly more energy-efficient than mechanical stirring (Herbolzheimer and Enrique, 2006). The hydrodynamics in a gas-liquid or gas-liquid-solid reactor are characterized by different flow regimes, mainly, the homogeneous transition, and heterogeneous regimes. The industrial interest for most processes is in the heterogeneous flow regime (Hyndman et al., 1997; Krishna et al., 1997). It is therefore extremely important to understand the different hydrodynamics regimes for the purpose of reactor design, operation, control, and scale-up. One of the approaches to identify the boundaries of the bubbly-transition-turbulent regimes is based on a sharp variation of the gas holdup (Zahradink and Fialova, 1996) or the drift flux (Zuber and Findlay, 1965; Vial et al., 2002) with respect to the superficial gas velocity. The dominate conditions that influence the hydrodynamics and mass and heat transfer behaviors include the superficial gas velocity, pressure, temperature, solid concentration and gas distribution. The superficial gas velocity is a

dominate factor that affects the gas holdup, and numerous experimental studies have been reported (Krishna et al., 1997; Degaleesan et al., 2001; Wang et al., 2004; Shaikh and Al-Dahhan, 2005). Electrolyte, salt, or system contaminants may exist inadvertently in slurry bubble columns in real industrial application. The presence of electrolyte or impurities was also found to increase the gas holdup (Hikita et al., 1980; Sada et al., 1984). (Ruzicka et al., 2005) reported that in spite of all the efforts aimed at the gas holdup studies, the information about the effect of solids on the flow regimes is very scarce and often, no attempt is made to specify the prevailing flow regime during the experiment. The hydrophobic/hydrophilic characteristic of solids is known to play a key role in many processes such as: wetting, flotation, enhanced oil recovery, cleaning technologies, super-hydrophobicity, liquid spreading, etc. (Jamialahmadi and Muller, 1991) demonstrated that an increase or decrease in gas holdup in an air-water system with the addition of solids depends on the nature of the solids. Hence, the effect of solids on transition velocity needs to be studied in terms of the nature of the solids (Sheikh and Al-Dahhan, 2007). (Ahmed et al., 2012) reported that hydrophilic particles could be converted to hydrophobic ones by surface treatment with hydrophobic aliphatic alcohols. Both the interfacial area a and the volumetric liquid-phase mass transfer coefficient $k_L a$ are considered the most important design parameters and bubble columns exhibit improved values of these parameters. For the design of a bubble column as a reactor, accurate data about bubble size distribution and hydrodynamics in bubble columns, mechanism of bubble coalescence and breakup as well as mass transfer from individual bubbles are necessary (Wilkinson et al., 1992). The correct estimation of bubble size is a key step for predicting successfully the mass transfer coefficients. Bubble diameters have been measured by photographic method (Ueyama et al., 1980), electroresistivity method (Fukuma et al., 1987), optical-fiber method and the chemical-absorption method (Letzel et al., 1999). Because of their simplicity, high accuracy and relatively low cost, optical fiber probes have been already used to determine local solids concentrations, size and distribution of bubbles and velocities in fluidized beds (Liu et al., 2003a, b). Jiang et al. (1995) applied the PIV technique to obtain bubble properties such as size and shape in a bubble column operated at high pressures. The goal of the present work was to increase the fundamental knowledge on the behavior of particle-to-bubble interactions in relationship to the physical properties of the catalyst particles, such as catalyst hydrophobicity, and catalyst concentration in slurry bubble columns. These investigations must be combined with the hydrodynamics of slurry bubble column i.e., gas hold-up, flow regimes and regime transitions and solid distribution. It is also the aim of

the present study to investigate the effect of solid properties on mass transfer coefficient and removal of environmental gaseous pollutants in a slurry reactor.

Materials and Methods

Figure 1 shows a schematic diagram of the experimental apparatus. The column is constructed of Plexiglas with inside diameter 0.13 m and height of 1.5 m. The column had (4) sample ports located – equally spaced-along the column height. An oil-free compressor (Model:V-0.12/8, 0.8MPa, 100L/min from Shimge Co.) was employed to supply air to the column. Air is introduced through 90 μ m porous sparger made of ceramic material and its flow rate is maintained using a calibrated air rota meter (Type: Roteck, Range: 0-100L/min). Distilled water with 0.15M NaCl solution was used as liquid phase. The liquid was confined into the column (no liquid throughput) and the clear liquid height was 0.9m for all experiments. In order to study the influence of the hydrophobicity of particles, two commonly used catalyst supports in heterogeneous catalyzed chemical reactors are used: silica and carbon particles in the loading range of (0-20%v/v).

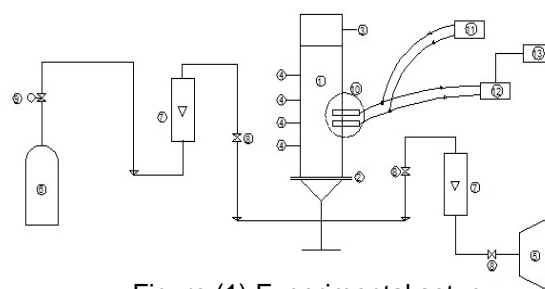
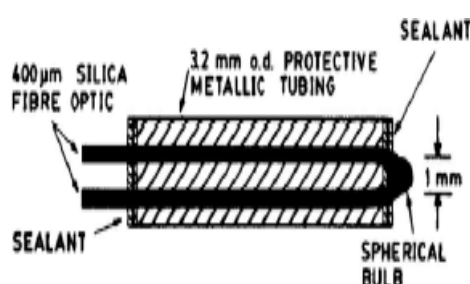


Figure (1) Experimental setup

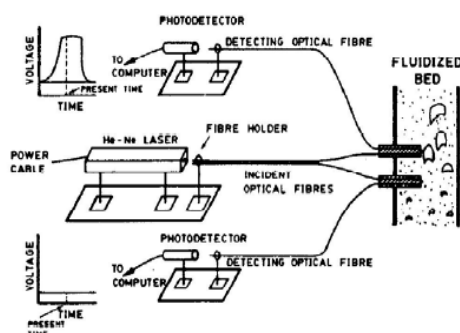
1-slurry bubble column, 2- porous gas sparger, 3- pressure taps, 4- sampling ports, 5- Oil-free air compressor, 6- CO₂ bottle, 7- Calibrated gas rota meter, 8- needle valves, 9- pressure regulator, 10- two parallel oriented optical fiber probes, 11-emitter, 12- receiver ,13- aquisition system with PC.

Experiments for mass transfer coefficient were carried out using a compressed bottle of CO₂ and a dual fiber-optical probe system as shown in Figure 1. For accurate measurements of bubble size and velocity, two homemade optical fiber probes (OFP) shown in Figure (2-a), based on the design utilized by Chabot et al. (1992), are going to be used with the probe tip located at 1/3 of the diameter of the slurry bed. In this system, bubble size and velocity measurements are obtained by correlation of voltage measurements at both OFPs. Optical probe selected was based on backscattering principle, with diameters of the fiber larger than the particle size. The measuring system showed in Figure (2-b), consists of an emitter which is illuminated by 750 nm

LED, a receiver with phototransistor, a passive splitter used for monitoring purposes, a RIFOCS power meter, and a data acquisition system in the PC. When particles in the emulsion phase pass in front of the probe, a high percentage of the emitted light is reflected, and the phototransistor responds with a high current, which is converted to a voltage signal at a resistance. In contrast, when a gas bubble passes, little light is reflected back to the probe and a low signal voltage is observed. Bubbles going through both optical fiber probes can be analyzed for determining its velocity and length. When the velocity and the time it takes the bubble to cross each probe is known, bubble length can also be obtained. The signal detected on each fiber was recorded with a digital oscilloscope (Model DS1052E, Rigol).



(a)



(b)

Figure (2) a- cross sectional view of the optical probe,

b- schematic diagram of the optical probe operating system. (Chabot et al, 1992)

To investigate effects of the solid particles (hydrophobic and hydrophilic) on the absorption rate of CO_2 in the slurry reactor, a pure gaseous CO_2 was used with 0.15 M electrolyte – water mixture. Mass transfer study was carried out in the Plexiglas column shown in Figure 1, with different superficial gas velocities and solid loadings. Temperature of the mixture is kept approximately constant at 25°C with a

deviation of $\pm 1^\circ\text{C}$. Samples from each run was taken after 1 hr, to reach steady-state conditions in the bulk of liquid. When CO_2 is absorbed into water a carbonate ion is formed. The rate of reduction of CO_2 is proportional to the concentration of hydroxyl ion (Pinset et al., 1956).



The concentration of carbonate ion was quantitatively identified by titration the sample against 0.5M NaOH solution.

The physical properties of solid particles and fluids used are given in Table 1 and Table 2 respectively.

Table 1 Physical properties of the catalyst support used in the present work

Property	Sand	Activated carbon
$d_p(\mu\text{m})^1$	120	110
$\rho_s(\text{kg/m}^3)^2$	2350	1300
$\epsilon_p(-)^3$	0.7	0.66
Pore diameter(nm)	8.5	9.1
$S_{\text{BET}}(\text{m}^2/\text{g})^4$	486	1864
Contact angle($^\circ$)	43	89.3

1- Measured using Beckman coulter LS 200.

2- Particle density measured using AccuPyc 1330 Pycnometer from micromeritics

3- Pore volume measured using SA 3100 from Beckman Inc.

4- BET area measured using SA 3100 from Beckman Inc.

5- Contact angle measure by VCA Optima from ACT products Inc.

Table 2 Physical properties of the fluids used (at 25°C , 1 bar)

fluid	$\rho_G(\text{kg.m}^{-3})$	$\mu_L(\text{Pa.s})$	$\sigma_L(\text{mN.m}^{-1})$	$\rho_L(\text{kg.m}^{-3})$
Air	1.24	-----	-----	-----
CO_2	1.904	-----	-----	-----
water	-----	$(1 \times 10^{-3})^a$	$(0.072)^a$	$(998)^a$
0.15M NaCl	-----	$(1 \times 10^{-3})^b$	$(0.071)^c$	$(1004)^d$

(a) Vandu and Krishna (2004); (b) Ozbek et al. (1977); (c) Mortimer (2008); (d) Perry (1963)

Theoretical Aspects

Gas holdup

In this study, the gas flow velocities have a wide range of variation (from 1 cm/s to 10 cm/s) which scanned the different flow regimes. The gas holdup was determined by measuring the aerated and quiescent height of liquid. The average fractional gas holdup ϵ_g is given by (Shah et al., 1982)

$$\varepsilon_g = \frac{(H_D - H_L)}{H_D} \quad (2)$$

Critical values

To determine critical values of gas holdup and superficial gas velocity, we followed the approach that had been commonly used in identifying the prevailing flow regime which is based on the concept of the drift-flux model, proposed by (Zuber and Findlay, 1964) and is expressed as follows:

$$\frac{u_g}{\varepsilon_g} = C_0 (u_g \pm u_l) + C_1 \quad (3)$$

Where $C_0 = \frac{(\varepsilon_g(u_g \pm u_l))}{(\varepsilon_g)(u_g \pm u_l)}$ is a parameter

related to radial uniformity of the gas holdup and

$$C_1 = \frac{\langle j_{gl} \rangle}{\langle \varepsilon_g \rangle}$$

is a parameter related to the bubble rise velocity. Because the radial profiles of the gas holdup are different in the homogeneous and heterogeneous regimes, the variation of C_0 with $u_g + u_l$ can be used to identify the flow regime transition as shown by (Zuber and Findlay, 1964), where was plotted against u_g (in batch liquid case).

$\frac{u_g}{\varepsilon_g}$ was identified as the bubble swarm velocity (Krishna, 2000).

Mass Transfer Coefficient

According to the bubble shape diagrams presented by Cliff et al. (1978) and Fan and Tsuchiya (1990) the bubbles formed under all operating conditions were oblate ellipsoids. To estimate volumetric liquid-side mass transfer coefficient, Nedeltchev & Schumpe (2007) proposed an accurate correlation for ellipsoidal bubbles by the following formula:

$$k_{La} = f_c \sqrt{\frac{AD_L R_{sf}}{\pi S_B}} \frac{f_B \cdot S_B}{A \cdot u_B} \quad (5)$$

Where R_{sf} is the rate of surface formation for oblate ellipsoidal bubbles (Nedeltchev et al., 2006a b).

$$R_{sf} = \pi u_g \left[\sqrt{\frac{l^2 + h^2}{2}} - \sqrt{\frac{(1-h)^2}{s}} \right] \quad (6)$$

f_c is a correction factor introduced by (Nedeltchev & Schumpe, 2007) accounts for the effect of the bubble wake and surface disturbance.

$$f_c = 0.124 Eo^{0.04} \left[\frac{\rho_g}{\rho_{gref}} \right]^{0.15} \quad (7)$$

f_B , and S_B are bubble formation frequency and bubble surface respectively.

D_L is the molecular diffusivity of solute into liquid solution estimated using Wilke and Chang correlation (Reid and Sherwood, 1977).

u_B is the bubble rise velocity which is estimated using eqn. 7 (Mainland and Welty, 1995).

$$u_B = \frac{L_{eff}}{\tau} \quad (8)$$

where L_{eff} and τ are the effective distance, between the bottom and top detecting fibers, and the time lag of the signals, respectively.

Chan et al. (1987) correlated the size of bubbles with the measured bubble length (l) as,

$$d_b = 1.43l \quad (9)$$

For calculating volumetric liquid-side mass transfer coefficient experimentally, an equation developed by Vandu and Krishna (2003) based on two film theory was used:

$$\frac{c_L}{c_L^*} = 1 - \exp \left[-\frac{k_{La}}{1 - \varepsilon_g} t \right] \quad (10)$$

The only unknown constant in equation (9) is k_{La} , which can be determined by a regression of equation (9) to the actual concentration data. With the aid of Statistica version 6.2 (2006), equation (9) can be solved to find k_{La} .

Results and discussion

Gas holdup

Effect of electrolyte

The variation of gas holdup against superficial gas velocity is shown in Figure 3 with and without the presence of electrolyte respectively. As expected, the gas holdup in the presence of electrolyte is higher compared to distilled water. This increase is attributed to the presence of surfactants which affect the bubble generation process, enhancing the creation of small bubbles and hindering coalescence which influences the rise velocity of bubbles. The rise velocity of a single bubble is decreased, resulting in a higher gas holdup.

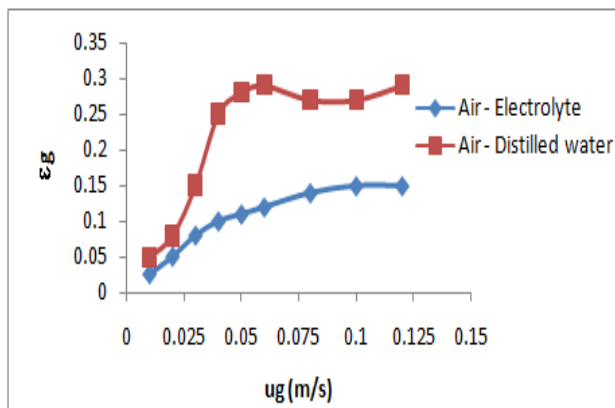


Figure (3) Variation of gas holdup vs. superficial gas velocity of solid free system

Effect of particles concentration and electrolyte

Figures (4 & 5) illustrate the variation of gas holdup in the presence of electrolyte and different concentrations of sand and activated carbon particles respectively. As can be seen, the gas holdup values increased with the solid content, at low solid loading, $C=0-3\%v/v$, and decreased at higher loading, $C>3\%v/v$ for both carbon and sand particles. This effect of solid loading on the gas holdup is interesting, since it indicates the presence of two competing mechanisms. First mechanism is the tendency of fine particles to rupture the gas-liquid interface of the bubble causing it to breakdown into smaller bubbles. With smaller bubbles the reduction of bubble rise velocity results in larger gas voidage. The second mechanism is to increase the "pseudo-viscosity" of the suspension which promotes the coalescence of bubbles resulting in an increase in bubble size and bubble rise velocity, consequently a decrease in a gas holdup. As can be seen the rate of decrease of gas holdup with increasing slurry concentration in the heterogeneous regime is lower compared to the rate of decrease of the gas holdup in the transition regime. The observation is in agreement with the results of (Krishna, 2000).

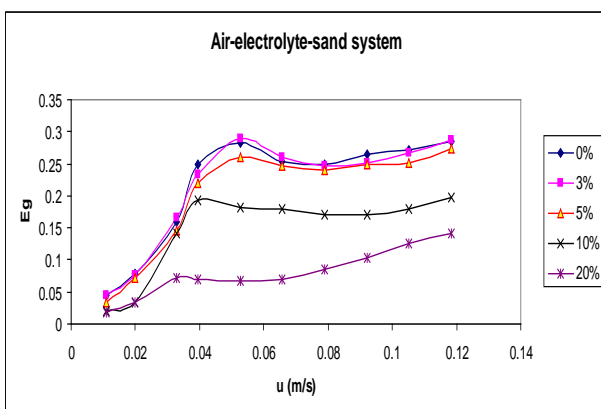


Figure (4) Variation of gas holdup vs. superficial gas velocity at different solid concentrations of sand particles

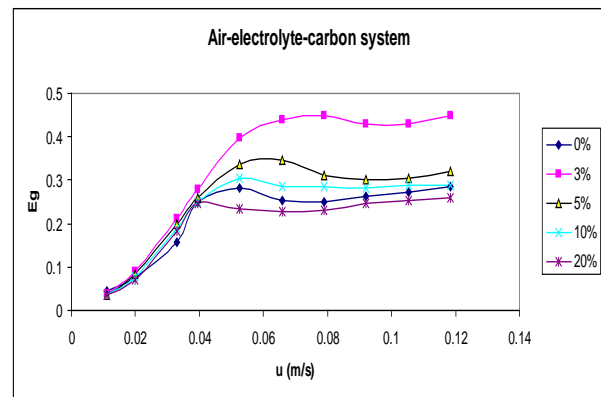


Figure (5) Variation of gas holdup vs. superficial velocity at different solid gas concentration of carbon particles

Influence of solid surface nature

Depending on the interfacial properties of the gas-liquid-solid system, particles tend to increase or reduce their concentration near the gas-liquid interface. The deposition at the bubble surface affects the original slip boundary condition. Stabilization of the surface then causes higher drag, hence lower rise velocity. The concentration differences along the interface can serve as a driving force for various processes and complicated electrokinetic phenomena can be encountered. Changes in the interfacial properties affect the tendency to coalescence and breakup. These effects will be strong in case of small particles, smaller than bubbles. Figures (4 & 5) depict the effect of solid surface nature (i.e., sand and activated carbon) on gas holdup. As can be seen, these two types of particles have different effects on gas holdup. Carbon particles increase the gas holdup in the SBC whereas sand particles decrease the gas holdup. This behavior of AC particles may be attributed to the adhesion of some microbubbles generated with micro porous gas sparger-of volume smaller than AC particles to the lyophobic surface. This phenomenon of bubble adhesion on AC particles leads to a decrease in the apparent density of the particle, which in turn is responsible for a larger bed expansion and smaller gas holdup compared with lyophilic particle system (i.e., sand in our present study). For bubbles of volume larger than hydrophobic particles (i.e., AC in our present study), a different phenomenon occurs which is the adhesion of the hydrophobic AC particles on the bubble-liquid interface causes higher drag, and consequently lower rise velocity of bubbles leading to an increase in gas holdup. These results suggest that the degree of hydrophobicity matters. Our results were also observed by (Armstrong et al., 1976; Tsutsumi et al., 1991)

Critical values

Each flow regime provides different phase behavior and mixing characteristics. If the bubble swarm

velocity, $u_{\text{swarm}} = ug/\epsilon_g$, are plotted against the superficial gas velocity, the relative minima in the curve may be taken to indicate the transition point of the studied regime (Krishna, 2000). Figures 6, 7, and 8 plot the effect of electrolyte-free solid, electrolyte-sand, and electrolyte-activated carbon on critical values of gas velocity respectively. As expected, all combinations used showed an impact on the transition point of the system in the following order, $u_{\text{el.}} > u_{\text{di}} > u_{\text{AC}} > u_{\text{sa.}}$. This may be attributed to the adhesion of the hydrophobic AC particles on the bubble-liquid interface causes higher drag, and consequently lower rise velocity of bubbles leading to an increase in gas holdup. Hydrophilic silica particles on the contrary decrease the regime transition point and also the gas hold-up. It was found that for low solid content, $C \leq 3\%v/v$, the solid load has a negligible effect on transition velocity with lower values of bubble swarm velocity. On the other hand, at larger content of solid, $C > 3\%v/v$, a gradual reduction in stability of bubbly flow regime took place. Table 3 shows a quantitated presentation of transition velocity as function of solid loading for carbon and sand particles according to Figures 7 and 8. Table 3 depicts the predominant effect of hydrophobic particles on the stability of bubbly flow regime over that of hydrophilic ones.

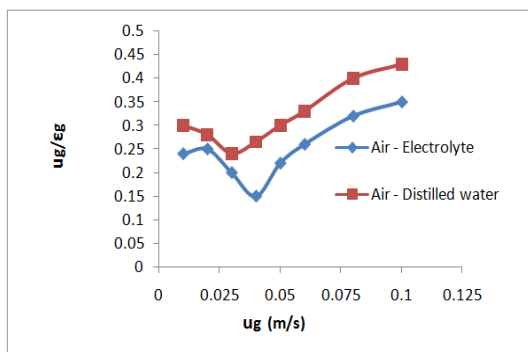


Figure (6) Variation of bubble swarm velocity vs superficial gas velocity for solid free system

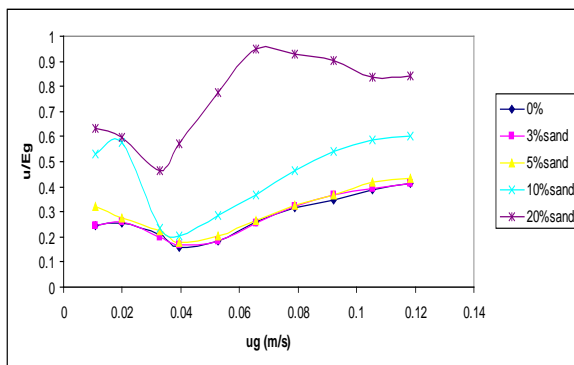


Figure (7) Variation of bubble swarm velocity vs. superficial gas velocity at different solid concentrations of sand particle.

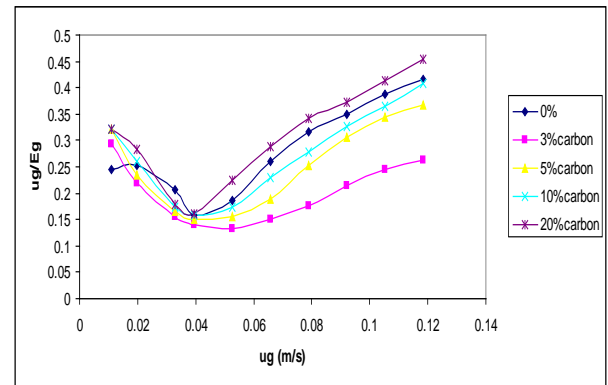


Figure (8) Variation of bubble swarm velocity vs. superficial gas velocity at different solid concentrations of carbon particles

Table 3 Effect of solid loading of wettable and non-wettable particles on critical gas velocity

Solid loading(%v/v)	Critical gas velocity(m/s) for sand particles	Critical gas velocity(m/s) for AC particles
0	0.0526	0.0526
3	0.0526	0.0789
5	0.0485	0.0657
10	0.0394	0.0586
20	0.0328	0.0394

Mass Transfer Coefficient

A typical measurement at both optical fibers (OFPs), P1 and P2 when a bubble is crossing by can be seen at Fig.9. The two signals represent responses of the upper and lower receiving fibers respectively. We can see that when a bubble passes by, a relatively little light is reflected, giving a low voltage signal. By analyzing the time-averaged of each signal, the time lag between the signals can be determined by using a polynomial fit to estimate the minimum point of voltage and equation (7) can be used to determine the bubble velocity. To get accurate average properties of bubbles, a long period of measurement was carried out. Results for AC and sand particles at solid loading of $3\%v/v$ are outlined in Table 4. Length of the bubble can be obtained from the contact time of the bubble with any of the receiving fibers, and by utilizing equation (7) along with the corresponding bubble rise velocity which listed in Table 3. Size of the bubble was determined by applying eqn. (8) with the measured length. Table 3 shows also the size of the bubbles corresponding to their rise velocities. The OFPs records of the relatively small size of the bubbles at the point where the probe tip was located is consistent with the relatively low values of rise

bubble velocity measured. Data outlined in Table 4 confirms the predominant effect of hydrophobic particles (i.e., AC) on size of the bubbles generated in the slurry bed and consequently on the gas holdup. Experimental results of Figure 10 show that the probe can also generate additional useful data, such as the distribution of the bubbles along the bed cross section in various operating conditions. Discreet regions can be seen in the histogram of Figure 10 this was attributed to crossing the light of the optical probes by solid particles. Figure 11 plots a comparison between k_La measured experimentally (eq. 9) and k_La predicted (eq.4). It is clear that by means of the OPFs technique the k_La values can be estimated reasonably well (within $\pm 18\%$).

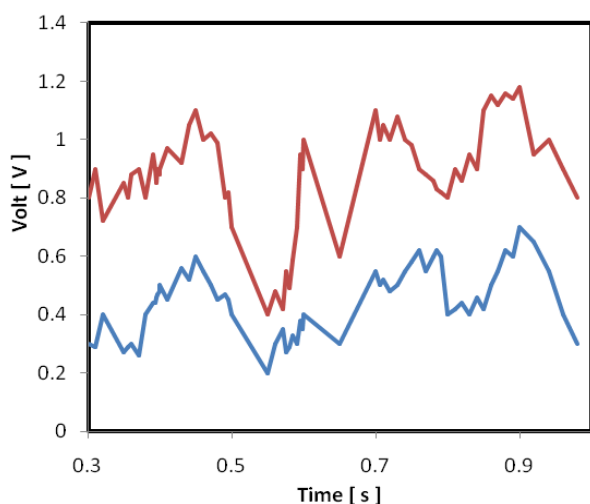


Figure (9) Output voltage measurements against time at bottom probe (upper signal) and top probe (lower signal)

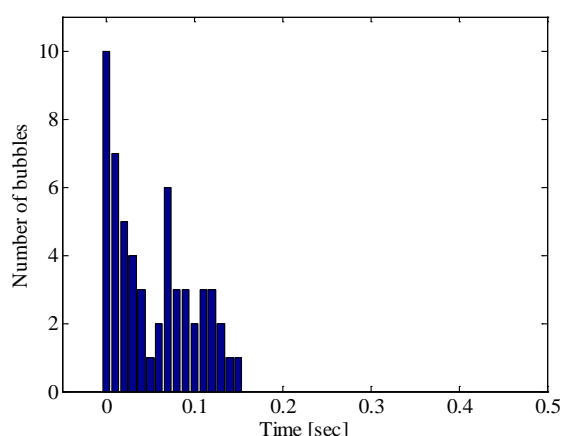


Figure (10) Histogram of bubble measurements in slurry bed (solid phase is AC particles).

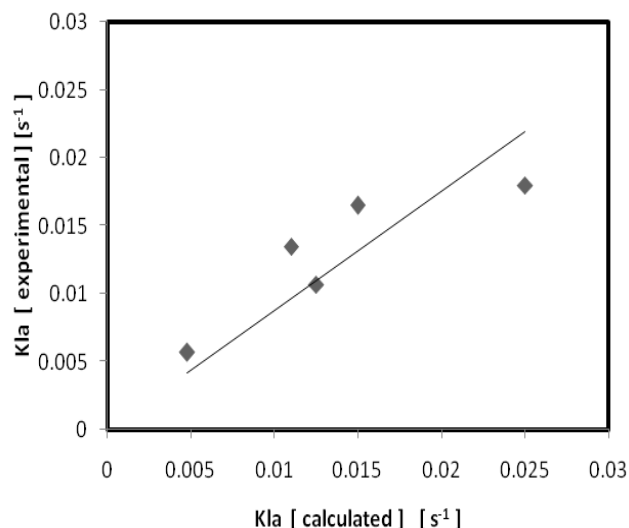


Figure (11) Experimentally measured against theoretical values of k_La (solid phase is AC particles).

Table 4 Set of measured time lag, bubble velocities and bubble size for AC and sand particles

AC particles			Sand particles		
Time lag (τ) (sec)	Bubble velocity (u_b) (cm/s)	Bubble size (d_b) (cm)	Time lag (τ) (sec)	Bubble velocity (u_b) (cm/s)	Bubble size (d_b) (cm)
2.81	4.53	0.166	2.04	5.21	0.24
2.09	5.16	0.129	1.92	5.84	0.35
1.82	6.27	0.49	1.78	6.85	0.71
1.75	7.11	0.78	1.71	7.96	1.14
1.64	8.02	0.97	1.52	8.97	1.37

CO₂ Removal

Figures 12 & 13 plot the performance of a batch slurry reactor in which a stream of pure gaseous CO₂ was bubbled through a bulk of 0.15M NaCl solution with different loadings of sand and carbon particles respectively. Samples for analysis were taken after one hour period of each run to reach steady state conditions. As can be seen from Figures 12 and 13, the conversion increased linearly in a steep rate until a relative maxima was reached, after then, CO₂ conversion started to decrease slightly. It is worth to note that, for each solid loading, the superficial gas velocity corresponding to maximum conversion obtained was approximately equal to the critical gas velocity estimated from Figures 7 & 8. This suggested that maximum CO₂ removal could be obtained at the boundaries of the bubbly-transition regimes. The trend in slight decrease of conversion at higher gas velocity may be attributed to the effect of bubble dynamics in turbulent regime. Large bubbles generated in the turbulent regime have

higher rise velocity, and consequently short contact time with liquid solution. Figures 12 & 13 depict the effect of particle hydrophobicity on CO₂ removal. As can be seen, slurry reactor loaded with non-wettable particles (i.e., AC) characterized by higher conversions of CO₂. This is mainly due to the surface nature and physical properties of AC particles which are presented in Table 1. Mass transfer experiments were carried out with pure gaseous CO₂ showed a behavior of removal in the same trend of increasing gas holdup with gas velocity. A noticeable removal of gaseous pollutants was observed for hydrophobic particles at solid loading of 3% v/v.

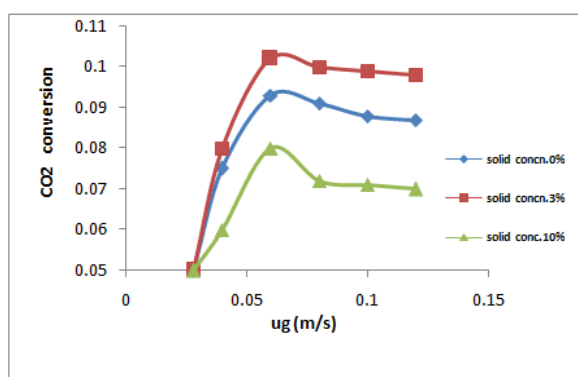


Figure (12) Effect of gas velocity on CO₂ concentration at various loadings of (sand) particles

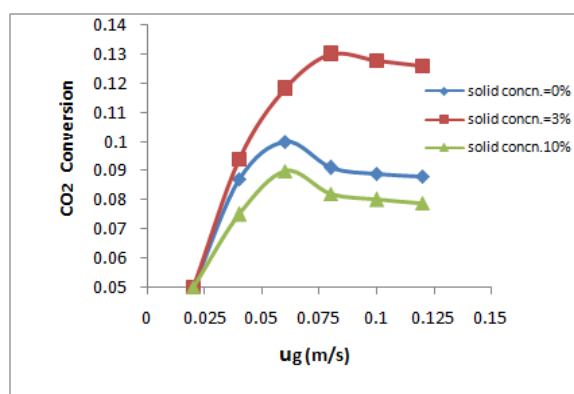


Figure (13) Effect of gas velocity on CO₂ concentration at different loading of AC particles

Empirical correlation

From the experimental results of CO₂ removal, the following power law based correlations were proposed (eq.10). Coefficients which were estimated using regression analysis technique are demonstrated in Table (5).

$$\text{CO}_2 \text{ conversion} = a_0 C^{a_1} u_g^{a_2} \quad (10)$$

Table 5 Statistical Evaluation of Fitting the Experimental Data with equation (10)

For sand					
	a_0	a_1	a_2	Correlation Factor(R^2)	variance
3%v/v	0.267099	-0.573761	1.115153	0.983	0.967
10%v/v	0.151108	-0.212422	0.698649	0.97	0.94
For AC					
3%v/v	0.12802	-1.13258	1.42051	0.9532	0.908
10%v/v	0.243139	-0.241215	0.896222	0.9849	0.97

Conclusions

The present work demonstrates and confirms the following,

- (i) The present study shows a noticeable effect of catalyst carriers on the hydrodynamics and mass transfer rate in a slurry reactor.
- (ii) The addition of active carbon, or silica particles at a solid loading $C \leq 3\%v/v$ to an aqueous solution of electrolyte, stabilizes the gas bubbles.
- (iii) It was found that catalyst supports (i.e., silica, and activated carbon), at concentrations greater than (3 %v/v) decrease the gas hold-up and shift the regime transition point to a lower gas velocity.
- (iv) Hydrobobic particles (i.e., AC particles) offers more gas holdup than hydrophilic ones (i.e., silica).
- (v) Experimental results show that the optical fiber probe is valid to use in slurry bubble column and can also generate useful data such as bubble rise velocity and bubble distribution.
- (vi) Volumetric liquid-side mass transfer coefficient can be predicted satisfactorily by means of optical fiber probes technique.
- (vii) Mass transfer experiments were carried out with gaseous CO₂ showed a behavior of removal in the same trend of increasing gas holdup with gas velocity. A noticeable removal of gaseous pollutants was observed for AC particles at solid loading of 3% v/v.

Aknowledgement

The authors are thankful to the Chemical Engineering Department- University of Technology- Baghdad, for providing space and facilities to carry out this work.

Nomenclature

- a specific interfacial area (referred to dispersion volume) (cm^{-1})
 A cross-sectional area of the reactor (cm^2)
 C solid concentration (%v/v).
 C_0 parameter in equation (3)
 C_1 parameter in equation (3)
 C_L concentration of solute (kgm^{-3})
 C_L^* equilibrium concentration of solute (kgm^{-3})
 d_b diameter of bubble (cm)
 D_L molecular diffusivity ($\text{cm}^2.\text{s}^{-1}$).

Eo Eötvös number
 f_B bubble formation frequency
 h height of an ellipsoidal bubble (cm)
 H_D Hight of dispersed slurry mixture (cm).
 H_L Hight of clear liquid (cm).
 $k_{L,a}$ Volumetric liquid-side mass transfer coefficient (s^{-1})
 l length (width) of an ellipsoidal bubble(cm)
 S_B bubble surface (cm^2)
 t time (s)
 u_g superficial gas velocity ($cm.s^{-1}$).
 u_{AC} critical superficial gas velocity for AC-electrolyte system ($cm.s^{-1}$).
 u_{dis} Critical superficial gas velocity for free solid-distilled water system ($cm.s^{-1}$).
 u_{el} Critical superficial gas velocity for free solid-elctrolyte system ($cm.s^{-1}$).
 u_l superficial liquid velocity ($cm.s^{-1}$).
 u_{sa} critical superficial gas velocity for sand-elctrolyte system ($cm.s^{-1}$).
 z axial distance along the column (cm).

Greek Letters

ϵ_g gas hold up (--).
 μ_L liquid viscosity (Pa.s)
 ρ_g gas density ($kg.m^{-3}$)
 ρ_{gref} reference gas density (air at ambient conditions) ($kg.m^{-3}$)
 ρ_L liquid density ($kg.m^{-3}$)
 σ_L liquid surface tension ($N.m^{-1}$)

References

Abid, M. F., A. A. Hadi, S. M. Ahmed, Hydrodynamic Characteristics Effect of Foam Control in a Three Phase Fluidized Bed Column, Journal of Petroluem Research and Studies, No. 6, pp 158-185, December 2012.

Armstrong, E. R., C. G. J. Baker, and M. A. Bergougnou, Effects of Solids Wettability on the Characteristics of Three-phase Fluidization, Fluidization Technology, 127, p.405, Hemisphere, Washington, DC (1976).

Babadi, F., and B.,Farhanieh, Characteristics of heat and mass transfer in vapor absorption of falling film flow on a horizontal tube,International Communications in Heat and Mass Transfer,Vol 32, 9, pp 1253-1265 (2005).

Chabot J., Lee S. L. P., Soria A., De Lasa H. I. (1992). "Interaction Between Bubbles and Fiber Optic Probes in a Bubble Column", *Can J Chem Eng*, 70: 61-68

Chan, I. E., Sisahtla, C., Knowlton, T.M., Effect of pressure on bubble parameters in gas-fluidized beds, Powder Technology, 53, 217- 245, 1987.

Clift, R.; Grace, J. R. & Weber, M. (1978), Bubbles, Drops and Particles, Academic Press, New York, U.S. A.

Degaleesan, S., M. Dudukovic, and Y. Pan, Experimental study of gas-induced liquid-flow structures in bubble columns, AIChE J., 47,9,1913-1931 (2001).

Fan, L.-S. & Tsuchiya, K, Bubble Wake Dynamics in Liquids and Liquid-Solid Suspensions, Butterworth-Heinemann Series in Chemical Engineering, Stoneham, U.S.A. (1990).

Fukuma, M.; Muroyama, K. & Yasunishi, A., Properties of Bubble Swarm in a Slurry Bubble Column, *J. Chem. Eng. Japan*, Vol. 20, 28-33(1987).

Herbolzheimer, E., and I. Enrique, Slurry bubble column, Patent US RE39,073 E, Apr. 18, 2006.

Hikita,H., Asai, S., Tanigawa, K., Segawa, K., and Kitao, M., Gas hold-up in bubble column, Chem. Eng. J., 20, 59 (1980).

Hyndman, C. L., Larachi, F., and Guy, C., Understanding gas-phase Hydrodynamics in Bubble column: a convective model based on kinetic theory, Chem. Eng. Sci. 1, 52, 63 (1997).

Jamialahmadi, M., and Muller-Steinhagen, H., Effect of solid particles on gas hold-up in bubble columns, Candian Journal of Chemical Engineering, 69, 390-393(1991).

Jiang, P.; Lin, T.-J., Luo, X. & Fan, L.-S., Flow Visualization of High Pressure (21 MPa) Bubble Columns: Bubble Characteristics, *Trans. Inst. Chem. Eng.*, Vol. 73, 269-274 (1995).

Katsuaki, I., Tong-Yen, W., K., Koide, and K., Hirodhi, The behavior of suspended solid particles in the bubble column, JCEJ, 1, 153-158 (1967).

Krishna, R., De Stewart, J. W. A., Ellenberger, J., Martina, G. B., and Maretto, C., Gas hold-up in slurry bubble columns: Effect of column diameter and slurry concentrations, AIChE J., 43, 311 (1997).

Krishna, R., A Scale-Up Strategy for a Commercial Scale Bubble Column Slurry Reactor for Fischer-Tropsch Synthesis, Oil and Gas Science and Techn.-Rev. IFP, Vol. 55, 359-393 (2000).

Letzel,H.M., J.C. Schouten, R. Krishna, C.M. van den Bleek, Gas holdup and mass transfer in bubble column reactors operated at elevated pressure. Chem Eng Sci 54: 2237–2246 (1999).

- Liu, J., J.R. Grace, X. Bi.,** Novel Multifunctional Optical-Fiber Probe: I. Development and Validation. *AIChE Journal* 49-6 1405-1420 (2003a).
- Liu, J., J.R. Grace, X. Bi.,** Novel Multifunctional Optical-Fiber Probe: II. High-Density CFB Measurements. *AIChE Journal* 49-6 1421-1432 (2003b).
- Mainland, M.E., J.R Welty,** Use Of Optical Probes To Characterize Bubble Behavior In Gas-Solid Fluidized Beds, *AIChE Journal* 41 (2) 223-228 (1995).
- Mortimer, R. G.,** Physical Chemistry, 4th edition, Elsevier Academic Press, Canada (2008).
- Nedeltshev, S. & Schumpe, A.,** Theoretical Prediction of Mass Transfer Coefficients in a Slurry Bubble Column Operated in the Homogeneous Regime, *Chem. & Biochem. Eng. Quarterly*, Vol. 21, 327-334 (2007).
- Nedeltshev, S.; Jordan, U. & Schumpe, A.,** Correction of the Penetration Theory Applied to the Prediction of kLa in a Bubble Column with Organic Liquids, *Chem.Eng. Tech.* , Vol. 29, 1113-1117 (2006a).
- Nedeltshev, S.; Jordan, U. & Schumpe, A.,** A New Correction Factor for Theoretical Prediction of Mass Transfer Coefficients in Bubble Columns, *J. Chem. Eng. Japan*, Vol. 39, 1237-1242 (2006b).
- Ozbek, H., J.A. Fair, and S. Phillips,** Viscosity of Aqueous Sodium Chloride Solutions From 0 - 150^o C, Presented Part at the American Chemical Society 29th Southeast Regional Meeting, Tampa, November 9-11, 1977.
- Perry, J.H.,** Chemical Engineering Handbook, 4th edition, McGraw-Hill, Inc., NY (1963).
- Pinset, B. R. W., L. Pearson, and F. J. W. Roughton,** The kinetics combination of carbon dioxide with hydroxide ions, *Trans .Faraday Soc.*, 52, 1512 (1956).
- Reid, R.C., and Sherwood, T.K.,** The properties of gases and liquids, 2nd edition, McGraw-Hill, New York (1977).
- Ruzicka, M. C., Mena, P.C., Rocha, F.A., and Drahos, J.,** Effect of solids on homogeneous-heterogeneous flow regime transition in bubble columns, *Chem. Eng. Sci.*, 60, 6013-6026 (2005).
- Sada, E., Katoh, S., and Yoshil, H.,** Performance of the gas-liquid bubble column in molten salt systems, *Ind. Eng. Chem. Process Des .Dev.*, 23, 151(1984).
- Shah, Y. T., Kellar, B. G., Godbole, S. P., and Deckwer, W. D.,** Design parameters estimation for bubble column reactors, *AIChE J.*, 28,353-379(1982).
- Sheikh, A., and Al-Dahhan, M.,** Characterization of the hydrodynamic flow regime in bubble columns via computed tomography.Flow Measurement and Instrumentation, 16(2-3), 91-98, (2005).
- Sheikh, A., and Al-Dahhan, M.,** A Review on Flow Regime Transition in Bubble Columns, *International Journal of Chemical Reactor Engineering*, Vol.5, Review R1, 1-68(2007).
- Tsutsumi, A., A., GhoshDastidar and L., Fan,** Characteristics of Gas-Liquid- Solid Fluidization with Nonwetable Particles, *AIChE Journal*, 37, 951-952.(1991).
- Vandu, C. O. and Krishna R.,** Gas Hold and Volumetric Mass Transfer Coefficient in a Slurry Bubble Column, *Chem. Eng. Tech.*, 26, NO.6 , 779-782 (2003).
- Vandu, C.O and Krishna R.,** Volumetric mass transfer coefficients in slurry bubble columns operating in the churn-turbulent flow regime, *Chemical Engineering and Processing* 43, 987–995 (2004).
- Vial, C., Poncina, S., Wild, G., and Midox, N.,** Experimental and theoretical analysis of the hydrodynamics in the riser of an external loop airlift reactor, *Chem. Eng. Sci.*, 57, 4745 (2002).
- Wang, T. F., Wang, J. F., Zahao, B., Ren, F., and Jin, Y.,** Local hydrodynamics in external loop airlift slurry reactors with and without resistance-regulating element, *Chem. Eng. Commun.*, 191, 1024 (2004).
- Wilkinson, P. M.; Spek A. P. & Van Dierendonck, L. L.,** Design Parameters Estimation for Scale-Up of High-Pressure Bubble Columns, *AIChE J.*, Vol. 38, 544-554(1992).
- Zahradink, J., and Fialova,M.,** The effect of bubbling regimes on gas and liquid phase mixing in bubble column reactors, *Chem. Eng. Sci.*,51, 2491 (1996).
- Zuber, N., and Findlay, J. A.,** Average volumetric concentration in two- phase flow systems, *J. Heat Transfer*, 87, 453 (1965).